SCANNING ACOUSTIC MICROSCOPY FOR NON-DESTRUCTIVE EVALUATION OF SUBSURFACE CHARACTERISTICS*

Jun Qu[1], Peter J. Blau[1], Albert J. Shih[2], Samuel B. McSpadden Jr.[1], George M. Pharr[1, 3] and Jae-il Jang[1,3]
[1]Metals and Ceramics Division, Oak Ridge National Laboratory, USA
[2]Department of Mechanical Engineering, University of Michigan, USA
[3]Department of Material Science & Engineering, University of Tennessee, USA

Abstract: Scanning Acoustic Microscopy (SAcM) has been widely used for non-destructive evaluation (NDE) in various fields including general material characterization, electronics, and biomedicine. SAcM uses high-frequency acoustic waves (60 MHz to 2.0 GHz) to reveal surface topography, subsurface features, and elastic properties of materials. With two unique advantages over other forms of material characterization, SAcM provides non-destructive subsurface imaging and offers the ability to visualize variations in elastic properties. These attributes make SAcM a valuable tool for near-surface material property characterization and flaw detection. The resolution of a SAcM can be as fine as 0.5 μm, much higher than that of conventional ultrasonic NDE, which is typically about 500 μm. Consequently, SAcM is more suitable for microstructural characterization and fine-scale flaw detection. The work presented here illustrates how a high-frequency scanning acoustic microscope can be used to identify subsurface damage, residual stress, and coating thickness of metallic, ceramic, semiconductor, and metallic glass materials and coatings. Specific cases discussed here are: (a) an extended subsurface crack in a silicon carbide wafer sliced by a diamond wire saw, (b) residual stresses and contact damage introduced by nanoindentation on a germanium wafer, (c) cracks and residual stress distribution around laser dimples on zirconia surfaces, (d) casting flaws and residual stresses in Zr-based bulk metallic glass material, and (e) the thickness of a Ni3Al coating. Although SAcM has provided impressive results in a variety of cases, some acoustic images are difficult to interpret because contrast derives from the combined effects of surface topography, subsurface features, material structures, and elastic properties.

Keywords: *Scanning acoustic microscopy, Subsurface damage, Residual stress, Coating, Ceramics, Semiconductors, Metallic glass*

1. Introduction

Traditional ways of assessing the damage beneath machined surfaces use destructive methods like etching, cross-sectional polishing, and scanning or transmission electron microscopy (SEM/TEM). By contrast, scanning acoustic microscopy is a non-destructive means to characterize subsurface damage and phase transformations in materials such as metals, coatings, composites, ceramics, and even metallic glass.

Scanning acoustic microscopy uses high-frequency acoustic waves to reveal surface topography, subsurface features, and elastic properties of materials [1-4]. The concept of SAcM is schematically illustrated in Fig. 1. Acoustic waves are produced by a transducer, pass through the coupling liquid (usually distilled water), and reflect from the focal plane (located at a distance 'z' below the specimen's surface). The reflected acoustic echoes from individual regions are detected during scanning and are used to build up images.

Compared to optical or scanning electron microscopy, which are limited to surface observations, the non-destructive SAcM method has two principal advantages: (1) acoustic waves can penetrate opaque materials to detect subsurface features, and (2) localized variations in elastic properties can be imaged. SAcM has been widely used for non-destructive evaluation in various fields including:

- General material characterization (subsurface flaw detection, detecting layer delamination, residual stress analysis, etc.)
- Electronics (integrated circuit packaging inspection, wafer evaluation, etc.)
- Biomedicine (studies of cells and tissues, etc.)

The spatial resolution of SAcM is proportional to the acoustic wavelength in the coupling fluid [1,2].

$$w \approx \frac{0.51}{N.A.} \cdot l_0 = \frac{0.51}{N.A.} \cdot \frac{v_0}{f} \qquad (1)$$

where w is the spatial resolution, l_0 is the acoustic wavelength in the coupling fluid, v_0 is the sound velocity in the coupling fluid, f is the acoustic frequency, and $N.A.$ is the numerical aperture.

* Research sponsored by the U.S. Department of Energy, Assistant Secretary for Energy Efficiency and Renewable Energy, Office of FreedomCAR and Vehicle Technologies, as a part of the High Temperature Materials Laboratory User Program, under contract DE-AC05-00OR22725 with UT-Battelle LLC.

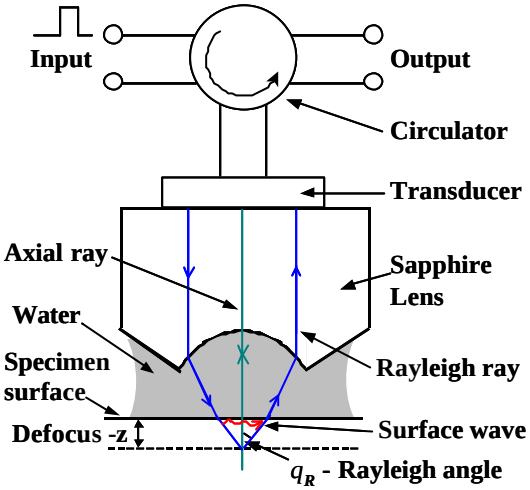

Fig.1 Schematic diagram of a scanning acoustic microscope.

The use of higher frequencies (i.e., lower wavelengths) provides better spatial resolution. Typical ultrasonic frequencies in medical imaging and traditional non-destructive evaluation (NDE) range between 2 and 10 MHz, but the SAcM uses much higher acoustic frequencies from 60 MHz to 2.0 GHz [1,2]. The resolution of a SAcM can be as fine as 0.5 μm (for 2.0 GHz lens with *N.A.* of 0.766), much higher than that of ultrasonic NDE whose lower limit is about 500 μm (for 10 MHz lens with *N.A.* of 0.153). Consequently, SAcM is more suitable than traditional ultrasonic NDE for microstructural characterization and fine-scale flaw detection. Due to their high attenuation, however, high-frequency acoustic waves lack the ability to penetrate materials deeply, and that restricts the imaging depth below the surface.

2. Instrument

The scanning acoustic microscope used in this study was Kraemer Scientific Instruments (KSI) SAM2000, as shown in Fig. 2. The KSI SAM2000 has working frequencies from 100 MHz to 2.0 GHz which, according to the manufacturer, is the highest working frequency of any commercially-available scanning acoustic microscope in existence. When using distilled water as the coupling fluid (v_0=1500 m/s), the resolution and maximum signal penetration depth of the instrument for typical metals and ceramics are listed in Table 1.

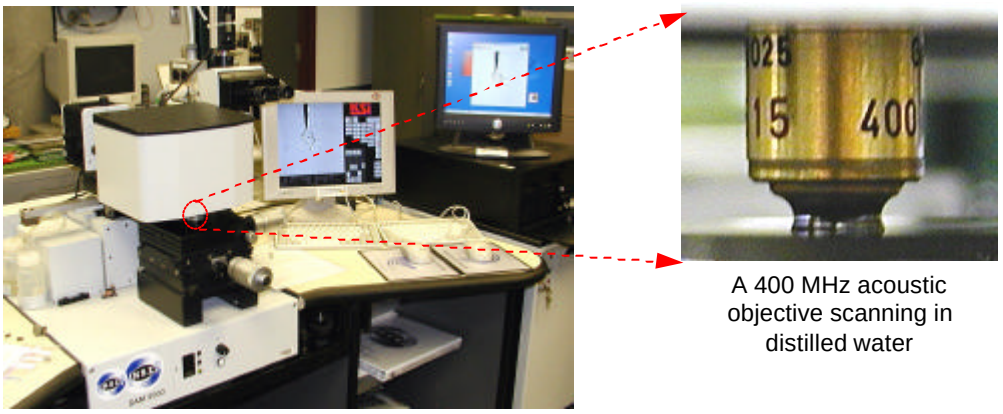

Fig.2. KSI SAM2000 scanning acoustic microscope.

Table 1. Resolution and maximum penetration of KSI SAM2000 at selected frequencies

Working frequency		100 MHz	200 MHz	400 MHz	1.0 GHz	2.0 GHz
Resolution (μm)		15	5	2	1	0.5
Max depth of penetration** (μm)	Metals	60~100	40~80	30~60	15~30	2~4
	Ceramics	40~80	25~65	20~50	10~20	1~3

** The penetration capability of the acoustic wave is highly dependent on material properties.

3. Case Studies

3.1 Detecting subsurface cracks in a silicon carbide wafer sliced by diamond wire saw

Single crystal silicon carbide (SiC) is an important semiconductor material used for the blue-color laser diodes in DVD readers/burners, energy efficient lighting, and power semiconductors. The fixed-abrasive, diamond wire saw process has been proposed for SiC wafer slicing since it offers low kerf loss, good dimensional control, high cutting speed, and low waste disposal cost; however, reducing residual surface and subsurface damage from the wire cutting process is an unsolved technical problem [5].

Fig. 3 compares optical and acoustic images of a single crystal silicon carbide wafer cut by a diamond wire saw. The wafer was sliced on a spool-to-spool, rocking motion, diamond wire saw (Millennium model, Diamond Wire Technology). Two cracks can be seen on the surface. The thick and long crack (labeled 'A' in Fig. 3) extends all way through the wafer thickness, but a thinner and shorter crack (labeled 'B' in Fig. 3) is only optically visible on the top surface of the wafer. These two cracks, claimed by the specimen provider to be from

an original defect of the wafer, were used to demonstrate the crack detection capability of the SAcM. Using a 400 MHz frequency and a 400 x 400 μm scanned area, acoustic images were obtained both on the surface and defocused 7 μm below the surface. The acoustic image is similar to the optical one, and provides little additional information. However, the acoustic image of the subsurface (Fig. 3(c)) reveals crack 'B' to be extended in the subsurface, much longer than it appears to be on the surface.

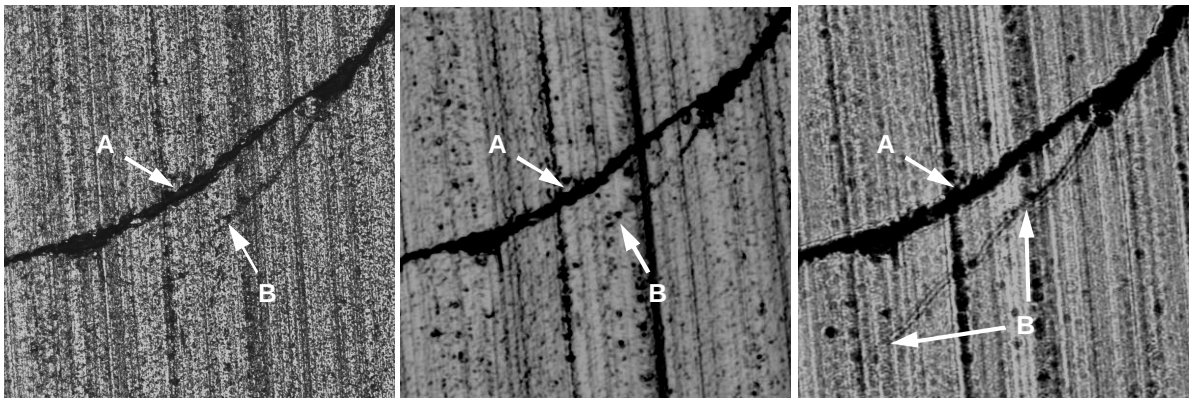

(a) Optical (b) Acoustic, on surface (c) Acoustic, 7 μm below surface

Fig.3. Optical and acoustic images of diamond wire saw cut silicon carbide wafer (image size: 400x400 μm).

3.2 Revealing the residual stresses and subsurface damage of nanoindentation on a germanium wafer

Indentation has been widely used as an experimental tool to probe the hardness and modulus of materials by means of load-displacement behavior. Nanoindentation applies very small loads, at the μN to mN level, to the specimen and generates indentation depths in the sub-μm to nm scale. This makes nanoindentation suitable and effective for measuring mechanical properties of thin films and small volumes of material.

Scanning electron microscopy has been widely used to identify the indent sizes and surface cracks for nanoindentation. In this study, the SAcM was able to reveal the residual stresses introduced by the indentation process. The SEM image in Fig. 4(a) shows 5x4 nanoindents on a germanium wafer surface. A cubecorner indenter with axis-to-face angle of 35.3° was used. For the indents from the top row to the bottom row, the maximum indentation loads and loading/unloading rates were 100, 80, 50, 50 mN, and 5, 5, 5, 2.5 mN/sec, respectively. The SAcM image generated by a 1.0 GHz acoustic objective is shown in Fig. 4(b). The contrast pattern surrounding the indents presents the residual stress field and/or subsurface contact damage. Darker areas imply higher stress. Apparently, higher load and loading/unloading rate caused higher residual stress level and larger stressed zone. Another set of nanoindents conducted by a Berkovich indenter (axis-to-face angle 65.3°) is shown in the SAcM image in Fig. 4(c). The maximum indentation loads were 700, 200,100, and 80 mN, for indents from the top to the bottom, respectively. It can be seen that the surrounding areas of the indents by 700 mN load were highly stressed. The fringes indicate subsurface cracks. The residual stress level dropped down quickly when low loads were applied. The clean field around the 80 mN-load indents indicates very low stresses and minimum subsurface damage.

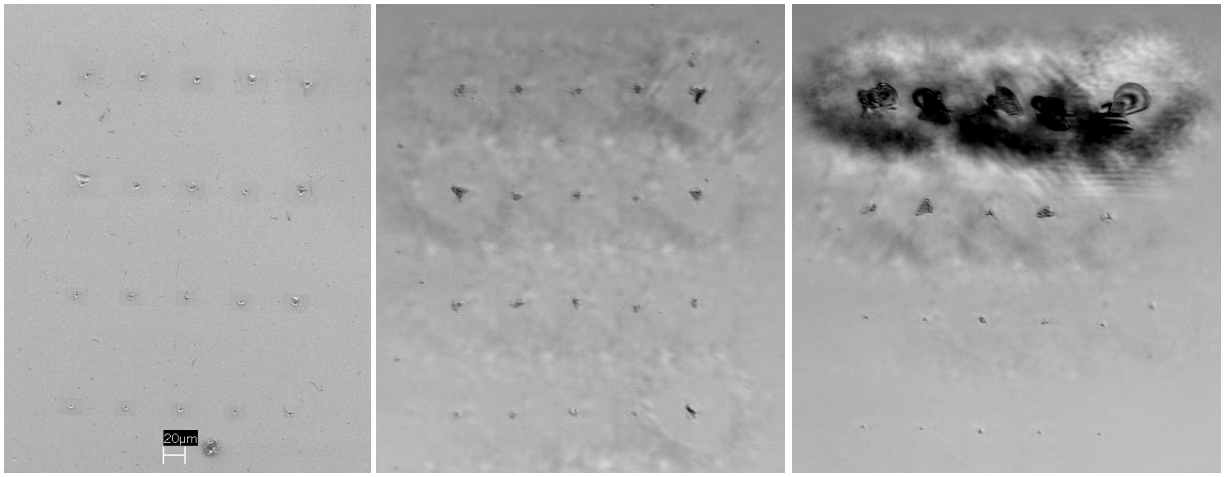

(a) SEM, cubecorner indents (b) SAcM, cubecorner indents (c) SAcM, Berkovich indents

Fig.4. Nanoindentation with different loads on a germanium wafer (image size: 400x400 μm).

3.3 Visualizing cracks and stresses in laser-dimpled zirconia

Patterns of shallow, round dimples have been applied by a laser surface treatment method to improve the lubricant flow characteristics on ceramic bearing surfaces [6,7]. The process of producing regular arrays of dimples on bearing surfaces results in thermal and mechanical stress gradients that can cause localized microstructural changes [8,9].

In this study, specimens of fine-grained, transformation-toughened zirconia (TTZ) were obtained in the form of 10 mm-diameter rods, approximately 30 mm long. In preparation for laser dimpling, flat areas were ground along the length of these rods. Surface treatment was conducted at Surface Technologies in Nesher, Israel using a 40 Watt, Nd:Yag Class 4, 3 kW laser with a programmable logic controller. The area fraction of dimples was determined by computer-aided image analysis to be about 29%.

SAcM and optical microscopy were used to characterize the surface and subsurface microstructures of the laser-dimpled TTZ. Fig. 5 shows optical and acoustic images of taper-polished cross sections. The plane of polish was slightly inclined (~ 5 degrees) with respect to the dimpled surfaces to better reveal near-surface structures. A SAcM working frequency of 1.7 GHz and a 200x200 μm scanned area were used. The circumferential rings visible inside the crater on the acoustic image are interference fringes caused by its concave shape. While both the optical and acoustic images show microcracks in the rim zone, more microcracks appear on the acoustic image, indicating the better crack detecting capability of SAcM. In addition, the acoustic image shows a contrast pattern around the crater. This contrast pattern may not be surface topography-related (since it is not evident in the optical image). Rather we suspect that it represents the distribution of residual stresses (and the attendant strains) caused by the laser dimpling process. Future X-ray diffraction-based measurements of residual stress are planned to support this hypothesis.

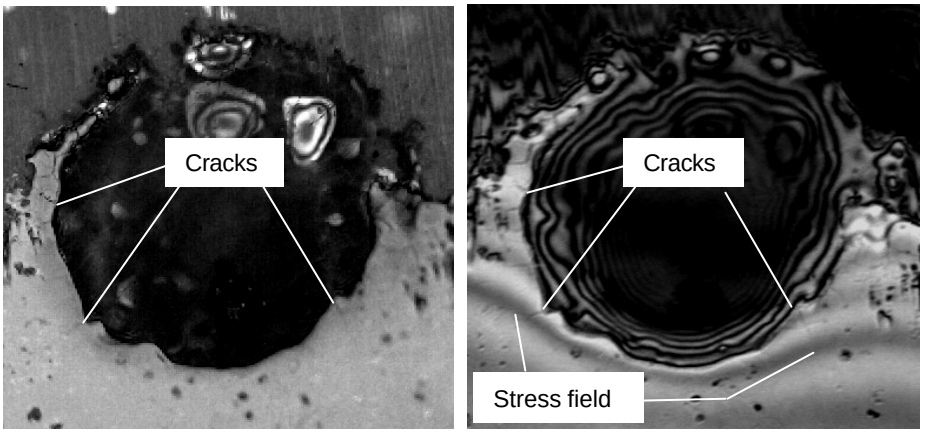

(a) Optical (b) Acoustic

Fig.5. Optical and acoustic images of a taper-polished cross-section of a laser dimpled surface of transformation-toughened zirconia (image size: 200x200 μm).

3.4 Detecting flaws and stresses in cast Zr-based bulk metallic glass

Bulk metallic glasses are amorphous alloys that display no long-range periodicity in their crystal structures. That feature imparts interesting properties to the materials. For example, zirconium-based bulk metallic glass, $Zr_{52.5}Ti_5Cu_{17.9}Ni_{14.6}Al_{10}$ [10], exhibits very high ultimate tensile strength (1900 MPa), an elastic strain limit (2%), and relatively low thermal conductivity (4 W/m-K). Casting is the most commonly used method for mass-producing bulk metallic glass parts, but casting flaws and residual stresses can adversely affect mechanical properties. In this example, SAcM was used to non-destructively characterize the flaws and stresses in a specimen of Zr-based bulk metallic glass material.

Fig. 6(a) shows an acoustic image (1.0 GHz acoustic frequency, 500 x 500 μm scanned area) of a polished surface of the Zr-based, cast bulk metallic glass specimen. There are only a few tiny casting flaws (dark specks) visible on the surface. No hint of the residual stress in the material shows on the stress-free surface. However, the defocused, subsurface image shown in Fig. 6(b) reveals additional casting flaws (patterns of dark spots) and residual stress fields (light and dark contrast pattern) within the bulk material. Further study is needed to verify the initial interpretation of the subtleties in this pattern.

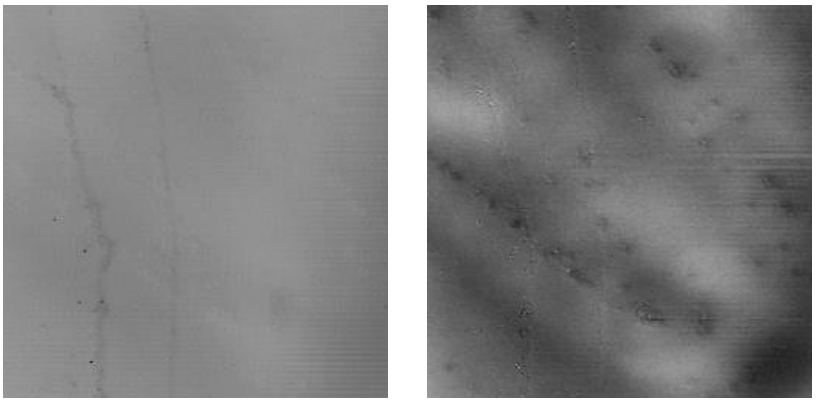

(a) Surface (b) Subsurface

Fig.6. Acoustic images of a cast, Zr-based bulk metallic glass alloy (image size: 500x500 μm).

3.5 Measuring the thickness of a Ni_3Al coating

Defocusing (focusing below the surface) has been used in the cases 3.1 and 3.4 to reveal the subsurface damage. This technique can also be used to detect the delamination or measure the thickness of a coating by focusing on the interface between the coated layer and the bulk material. The coating thickness can be calculated by the following equation:

$$t = \left| z \cdot \frac{v_{water}}{v_{coating}} \right| \quad (2)$$

where v_{water} and $v_{coating}$ are the sound velocities of the acoustic longitudinal wave in the coupling fluid (water) and the coating material, respectively, and z is the physical displacement of an acoustic objective moving the focus from the coating surface to the interface.

A nickel-aluminide (Ni_3Al) coated Ni alloy specimen was examined by SAcM, as shown in Fig. 7. The surface image (Fig. 7(a)) clearly shows the grain boundaries of the nickel-aluminide coating. The existence of the Ni_3Al microstructure in the subsurface image in Fig. 7(b) indicates the focal layer inside the coating material. The Ni_3Al microstructure started fading off at 105 μm defocus and eventually disappeared at z = 110 μm (Fig. 7(c)). This indicated the focal point reached the diffusion layer (interface). Given sound velocities in water and Ni_3Al are roughly 1500 and 7500 m/s, respectively, the thickness of the nickel-aluminide coating can be calculated, about 22 μm.

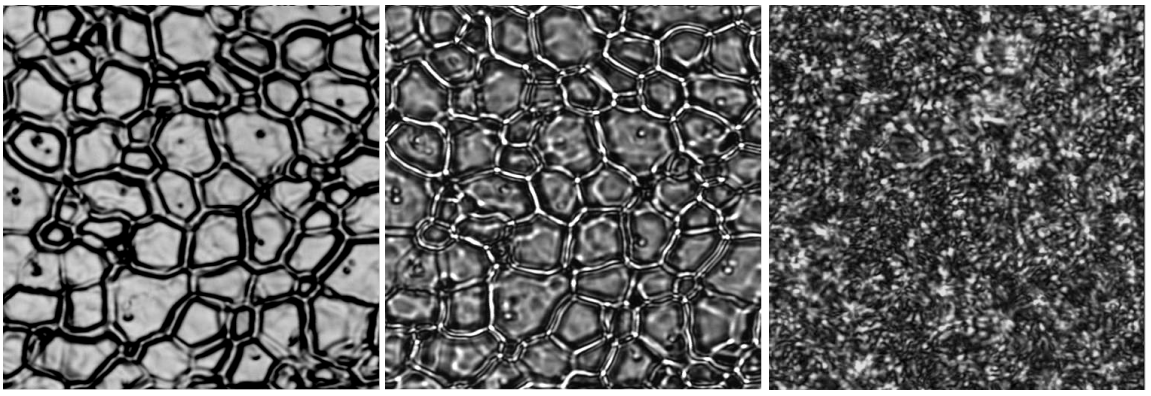

(a) Coating surface (z = 0) (b) Inside coating (z = 30 μm) (c) Interface (z = 110 μm)

Fig.7. Acoustic images of a Ni_3Al coating on Ni alloy (image size: 500x500 μm).

4. Summary

Scanning acoustic microscopy was used to non-destructively assess the subsurface damage and residual stresses introduced by various processes on metals, ceramics and metallic glass materials. Extended subsurface cracking was detected on a silicon carbide wafer sliced by a diamond wire saw. Casting flaws were observed underlying the surface of a Zr-based bulk metallic glass specimen. The unique ability of the acoustic microscope to visualize local variations in elastic properties enabled residual stress fields to be mapped on nanoindented germanium, laser-dimpled zirconia, and within cast bulk metallic glass. Scanning acoustic microscopy was particularly helpful in detecting the coating delamination and measuring the coating thickness.

The contrast in SAcM images arises from different sources than are responsible for optical or electron microscope images. SAcM contrast derives from localized changes in the propagation and attenuation of elastic waves. Surface topography, subsurface flaws, microstructural discontinuities, and stress (strain) gradients like those shown in the foregoing examples can all produce contrast changes. Although some of the

images resemble optical views, SAcM images contain other types of information, and sorting them out requires careful interpretation.

Acknowledgements

Research sponsored by the U.S. Department of Energy, Assistant Secretary for Energy Efficiency and Renewable Energy, Office of FreedomCAR and Vehicle Technologies, as a part of the High Temperature Materials Laboratory User Program, under contract DE-AC05-00OR22725 with UT-Battelle LLC.

References

[1] A. Briggs, *An Introduction to Scanning Acoustic Microscopy*, Oxford University, 1985.

[2] A. Briggs, *Acoustic Microscopy*, Clarendon, 1992.

[3] A. Briggs (Ed.), *Advances in Acoustic Microscopy*, Vol. 1, Kluwer, 1995.

[4] A. Briggs, Arnold W. (Ed.), *Advances in Acoustic Microscopy*, Vol. 2, Plenum, 1996.

[5] C.W. Hardin, J. Qu, A.J. Shih, "Fixed Abrasive Diamond Wire Saw Slicing of Single Crystal Silicon Carbide Wafers," Materials and Manufacturing Processes, 19, No. 2, 2004: 357–369.

[6] K-H. ZumGahr, J. Schneider, " Surface modification of ceramics for improved tribological properties," *Ceramics International*, 26(4), 2000: 363-370.

[7] X. Wang, K. Kato, K. Adachi, K. Aizawa, "The lubrication effect of micro-pits on parallel sliding faces of SiC in water," *Lubrication Engineering*, 58(8), 2002: 27-34.

[8] I. Black, " Experimental detection of micro-cracks during the CO2 laser machining of ceramics," *Lasers in Engineering*, 11(1), 2001: 29-45.

[9] M.F. Modest, "Minimization of elastic thermal stresses during laser machining of ceramics using a dual-beam arrangement," *Journal of Laser Applications*, 13(3), 2001: 111-117.

[10] C.T. Liu, L. Heatherly, D.S. Easton, C.A. Carmichael, J.H. Schneibel, C.H. Chen, J.L. Wright, M.H. Yoo, J.A. Horton, A. Inoue, "Test environments and mechanical properties of Zr-base bulk amorphous alloys," *Metallurgical And Materials Transactions A*, 29A, 1998: 1811-1820.

Contact Info:

Jun Qu
Metals & Ceramics Division
Oak Ridge National Laboratory
P.O. Box 2008, MS 6063
Oak Ridge, TN 37831-6063, USA
1-865-5769304, 1-865-5746918 (fax)
Email:qujn@ornl.gov